



Communication

High Precision Measurements of Resonance Frequency of Ozone Rotational Transition $J = 6_{1,5}-6_{0,6}$ in the Real Atmosphere

Mikhail Yu. Kulikov ^{*}, Alexander A. Krasil'nikov, Mikhail V. Belikovich , Vitaly G. Ryskin, Alexander A. Shvetsov , Natalya K. Skalyga, Lev M. Kukin and Alexander M. Feigin

A.V. Gaponov–Grekhov Institute of Applied Physics of the Russian Academy of Sciences, 46 Ulyanov Str., 603950 Nizhny Novgorod, Russia; alakras@ipfran.ru (A.A.K.); belikovich@ipfran.ru (M.V.B.); rys@ipfran.ru (V.G.R.); shvetsov@ipfran.ru (A.A.S.); sknata@ipfran.ru (N.K.S.); epk41@mail.ru (L.M.K.); feigin@ipfran.ru (A.M.F.)

* Correspondence: kulm@ipfran.ru

Abstract: Ground-based passive measurements of downwelling atmospheric radiation at ~ 110.836 GHz allow extracting the spectra of ozone self-radiation (rotational transition $J = 6_{1,5}-6_{0,6}$) coming from the low stratosphere–mesosphere and retrieving vertical profiles of ozone concentration at these altitudes. There is a notable (several hundred kHz) ambiguity in the determination of the resonance frequency of this important ozone line. We carried out long-term ground-based measurements of atmospheric microwave radiation in this range using upgraded apparatus with high technical accuracy and spectral resolution (~ 12 kHz). The obtained brightness temperature spectra allowed us to determine the frequency of this ozone line to be $110,835.909 \pm 0.016$ MHz. We verified that the Doppler frequency shift by horizontal wind as well as the variations of the tropospheric absorption had little effect on the obtained result. The found value was 131 ± 16 kHz less than that measured in the laboratory and differed from modern model calculations. At the same time, it was close to the results of early semiempirical calculations made more than 40 years ago. The applications where precise knowledge about the resonance frequency of this ozone line can be important were discussed in this paper.

Keywords: ozone; rotational transitions; millimeter wave spectrum; microwave spectroradiometer; stratosphere; mesosphere



Citation: Kulikov, M.Y.; Krasil'nikov, A.A.; Belikovich, M.V.; Ryskin, V.G.; Shvetsov, A.A.; Skalyga, N.K.; Kukin, L.M.; Feigin, A.M. High Precision Measurements of Resonance Frequency of Ozone Rotational Transition $J = 6_{1,5}-6_{0,6}$ in the Real Atmosphere. *Remote Sens.* **2023**, *15*, 2259. <https://doi.org/10.3390/rs15092259>

Academic Editors: Alexander Kokhanovsky and Dmitry Efremenko

Received: 3 March 2023

Revised: 21 April 2023

Accepted: 22 April 2023

Published: 25 April 2023



Copyright: © 2023 by the authors. Licensee MDPI, Basel, Switzerland. This article is an open access article distributed under the terms and conditions of the Creative Commons Attribution (CC BY) license (<https://creativecommons.org/licenses/by/4.0/>).

1. Introduction

It is well-known that, due to rotational transitions, the self-radiation of atmospheric ozone in the microwave range is a useful proxy enabling retrieval of vertical distribution of ozone at altitudes of the stratosphere and the mesosphere. Over the last few decades, the spectra of downwelling atmospheric radiation at around ~ 110.8 GHz ($J = 6_{1,5}-6_{0,6}$) and ~ 142.2 GHz ($J = 10_{1,9}-10_{0,9}$) were measured by a number of ground-based passive radiometers (ozonometers). The measurement results are then used to retrieve ozone profiles (see, for example, [1–4]). Retrieval procedures exploit different methods. The commonly used optimal estimation methods [5] are based on the Bayesian approach, i.e., probabilistic description of the measurement system. The approach considers the posterior probability density of possible ozone profiles, given the measurement together with the description of its error statistics (noise magnitude), the radiative transfer model, and available a priori information. The most probable ozone profile corresponding to the maximum of this probability density is usually chosen to be the retrieval result. Error analysis provides the estimate of profile uncertainty. The obtained data are used to study the local evolution of middle atmospheric ozone with different time scales. Special attention is paid to the ozone depletion in polar regions, long-term trends at different latitudes [6], oscillations with different time-space scales [7,8], and ozone response to disturbed atmospheric condi-

tions, such as seasonal redistribution of the middle atmosphere accompanied by sudden stratospheric warnings [9,10].

Early radiometers were equipped with filter banks of several tens of broadband channels providing the spectral resolution from several hundred kilohertz to several tens of megahertz. Nowadays, the improved apparatus sensitivity as well as the use of modern digital spectrum analyzers, for example, based on the fast Fourier transform allow increasing the resolution up to several tens of kilohertz or better, which opens up new applications of ozonometers for studying atmospheric characteristics. In particular, the central part of the ozone emission line is affected by horizontal wind via the Doppler effect. Thus, using its ultra-high-resolution measurements (up to several kilohertz) one can retrieve horizontal wind profiles at altitudes from the middle stratosphere to the upper mesosphere [11]. Moreover, high resolution makes it possible to determine the frequency position of the corresponding ozone line with better precision. In particular, Forkman et al. [12] presented a new radiometer for simultaneous observations of CO and O₃ lines at 115.3 GHz and 110.8 GHz, respectively, with a resolution of 25 kHz. Based on the measurements, the authors concluded that the O₃ line position is shifted by 117 ± 50 kHz from the generally accepted value. In this work, we report the results of the first high-precision atmospheric measurements of the resonance frequency of the O₃ line at 110.8 GHz.

The paper has the following structure. Section 2 summarizes current knowledge about this line position. Section 3 contains a description of the used apparatus, its upgrading and laboratory testing, the peculiarities of the performed measurements, and processing of the obtained data. The main results are presented in Section 4. Section 5 contains a short discussion and possible applications of the high-precision measurements. The Section 6 ends the paper.

2. O₃ Line at 110.8 GHz

The previously obtained data on this line position are summarized in Table 1. Only laboratory measurements [13] where the resonance frequency was found to be 110,836.040 MHz are known today. This value was cited in many papers (see, e.g., [1,2]) where ground-based ozonometers were applied to study the middle atmospheric ozone. As mentioned, Forkman et al. [12] measured simultaneously the CO and O₃ lines at 115.3 GHz and 110.8 GHz with a resolution of 25 kHz. Comparing the measured and simulated spectra in each range, they found that both spectra of the CO line were consistent, whereas there was a shift (117 ± 50 kHz) between the spectra of the O₃ line. In other words, Forkman et al. [12] discovered this shift using the CO line position as a reference point. The second column in Table 1 presents the results of early semiempirical calculations [13–16]. These data show lower values shifted from the ones measured in the laboratory [13] by 120–1040 kHz. Modern databases and models (see the third column in Table 1) present the values closer to those measured in the laboratory or higher by 230 kHz. Thus, one can conclude that there is a notable ambiguity in the resonance frequency of this important ozone line.

Table 1. Current knowledge about the resonance frequency of ozone transition $J = 6_{1,5}-6_{0,6}$.

Measured Values	Early Models	Modern Databases and Models
110,836.040 MHz [13]	110,835 MHz [14]	110,836.030 MHz [17]
110,835.923 \pm 0.05 MHz [12]	110,835.87 MHz [13]	110,836.040 MHz [18]
	110,835.92 MHz [15]	110,836.270 MHz [19]
	110,835.9 MHz [16]	110,836.270 MHz [20]
		110,836.040 MHz [21]

3. The Apparatus and Experimental Procedures

Our spectroradiometer [22] was based on the classical heterodyne principle of receiving and analyzing millimeter wave radiation (see Figures 1 and 2). Originally, it consisted of an input horn antenna with a beam width of $\sim 4^\circ$ at 110.836 GHz, a self-made calibration system based on compact electrically controlled etalon (modulator–calibrator [23]), a low-noise amplifier with a gain of over 20 dB operating in the 109–113 GHz frequency range with a noise temperature of ~ 1000 K (Mi-Wave, St. Petersburg, FL, USA), two cascades of frequency conversion, and a fast-Fourier-transform digital spectrum analyzer (ACQIRIS)—AC240 with a bandwidth of 1 GHz, 16,384 channels of which provided a spectrum resolution of ~ 61 kHz. Each cascade of frequency conversion included a local oscillator (LO), a mixer, and an amplifier of intermediate (differential) frequency. The LOs were tuned to frequencies of ~ 104.4 GHz and ~ 5.935 GHz. The first cascade converted the signal of atmosphere (or calibrator etalon) to the 6.036–6.836 GHz range, whereas the second one converted the signal of atmosphere (or calibrator etalon) to the 101–901 MHz range. After that, it was analyzed by the digital spectrum analyzer, so that the ozone line maximum corresponded to a frequency of ~ 501 MHz.



Figure 1. Spectroradiometer of the Institute of Applied Physics. The laptop display demonstrates the measured spectrum of downwelling atmospheric radiation at around ~ 110.836 GHz.

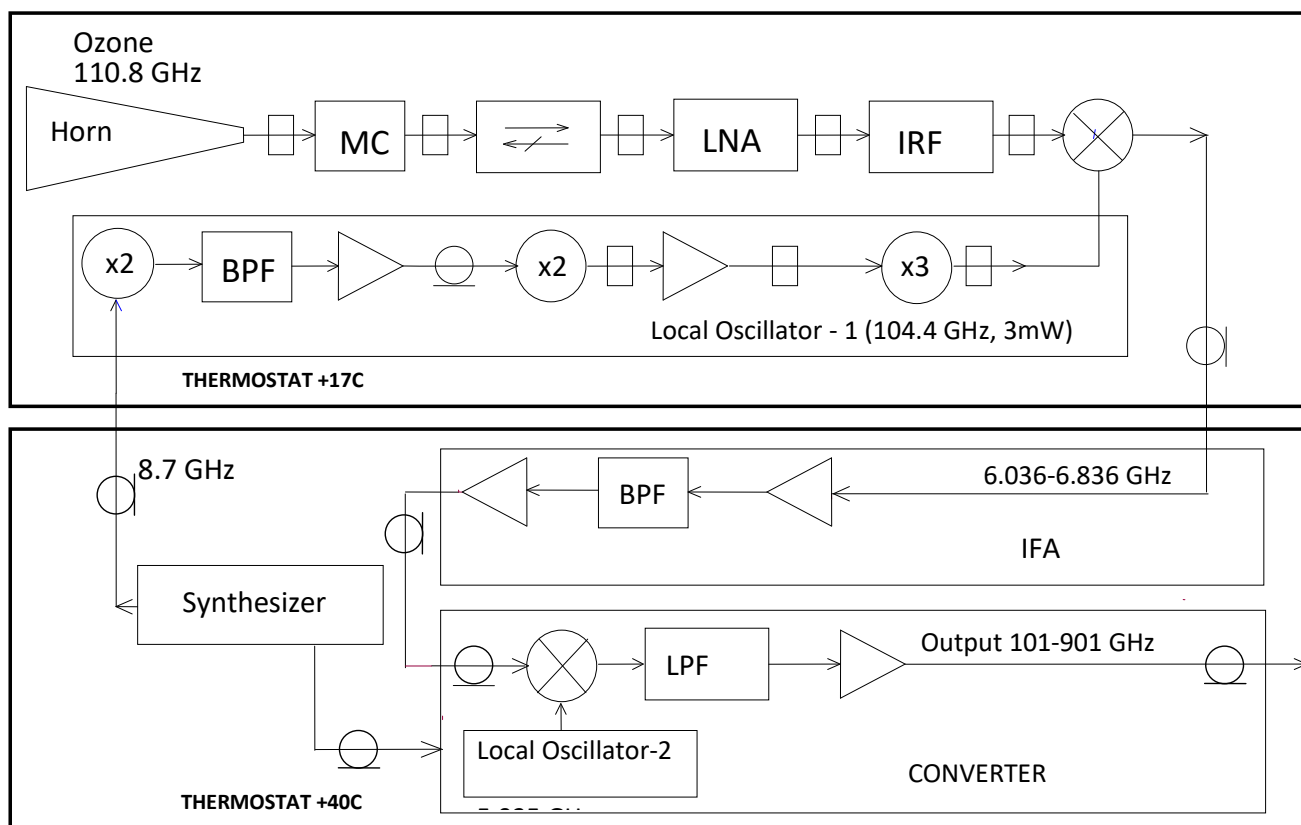


Figure 2. Block-diagram of the spectroradiometer. MC is a modulator–calibrator, LNA is a low-noise amplifier, IRF is an image reflection filter, BPF is a band-pass filter, IFA is an intermediate frequency amplifier, and LPF is a low-pass filter.

Recently, the ozonometer was upgraded as follows. First, we reduced the bandwidth of the digital spectrum analyzer from 1 GHz to 200 MHz while maintaining the number of channels, so that the spectrum resolution of measured spectra became ~ 12.2 kHz. Second, the third cascade of frequency conversion was added to shift the signal to the range of 30–90 MHz and to obtain the maximum of the ozone line corresponding to the frequency of ~ 61 MHz. Third, we determined the frequency and spectrum width of the signal after the second and third LOs. We used a generator of etalon signals (R&S[®]SMB100A, Munich, Germany) with an external frequency standard at 10 MHz (Pendulum GPS-12RG controlled by GLONASS/GPS navigation satellite systems) as a reference signal source with increased stability and spectrum purity. The claimed frequency stability was better than 10^{-11} . A monochromatic signal with an initial frequency of 11,083.600 MHz multiplied by 10 was sent to the ozonometer antenna. The output signals at intermediate frequencies after each LO were measured with a KEYSIGHT-N9010B signal analyzer with an accuracy of 1 Hz. Long-term measurements revealed that the frequency after the third LO was equal to 61.060996 MHz with frequency stability much better than 1 kHz. Thus, the summarized frequency of all three LOs was equal to 110,774.939004 MHz with a possible error much less than the improved spectrum resolution of the ozonometer.

We carried out two series of continuous measurements of the central part of the atmospheric ozone rotational transition $J = 6_{1,5}-6_{0,6}$ over Nizhny Novgorod (56.2°N , 44°E) during the spring of 2019 and autumn–winter of 2019–2020. To obtain a sufficient intensity of ozone radiation at 110.836 GHz, the measurement angle was 20° above the horizon. To exclude the Doppler shift of this emission line by the zonal wind, the direction of receiving atmospheric radiation was oriented due north. Note that, usually, meridional winds are remarkably less than zonal winds. Nevertheless, we estimated a possible Doppler shift by the meridional wind with the use of the microwave propagation model [21]. Typical

profiles of ozone concentration over the measurement site during a year were taken from the Aura MLS data [24]. The meridional wind profiles data are from the well-known 3D model of the dynamics of the middle atmosphere CMAM (Canadian Middle Atmosphere Model) [25,26].

Almost all successive atmospheric spectra of the brightness temperature were recorded with a signal accumulation time of 1 h. For improving the signal-to-noise ratio, we used one-day or multi-day averaging. It is well-known that the ozone radiation coming from the middle atmosphere is modified essentially by absorption in the troposphere (mainly due to water vapor) which may vary with a time scale of several hours or less. Therefore, before averaging, we used spectra filtering by a tropospheric attenuation coefficient (TAC) not higher than a certain selected level. This coefficient showed how many times the amplitude of ozone line decreased due to tropospheric absorption. The center frequencies of the averaged spectra were found by parabolic approximation within a 400 kHz range.

4. Results

Figure 3 demonstrates an example of the brightness temperature spectrum of atmospheric ozone obtained by averaging the data measured during two weeks of April 2019. This spectrum was compared with the spectrum of the reference monochromatic signal at the frequency of 110,836.040 MHz corresponding to the laboratory value of the resonance frequency of ozone transition $J = 6_{1,5}-6_{0,6}$ [13].

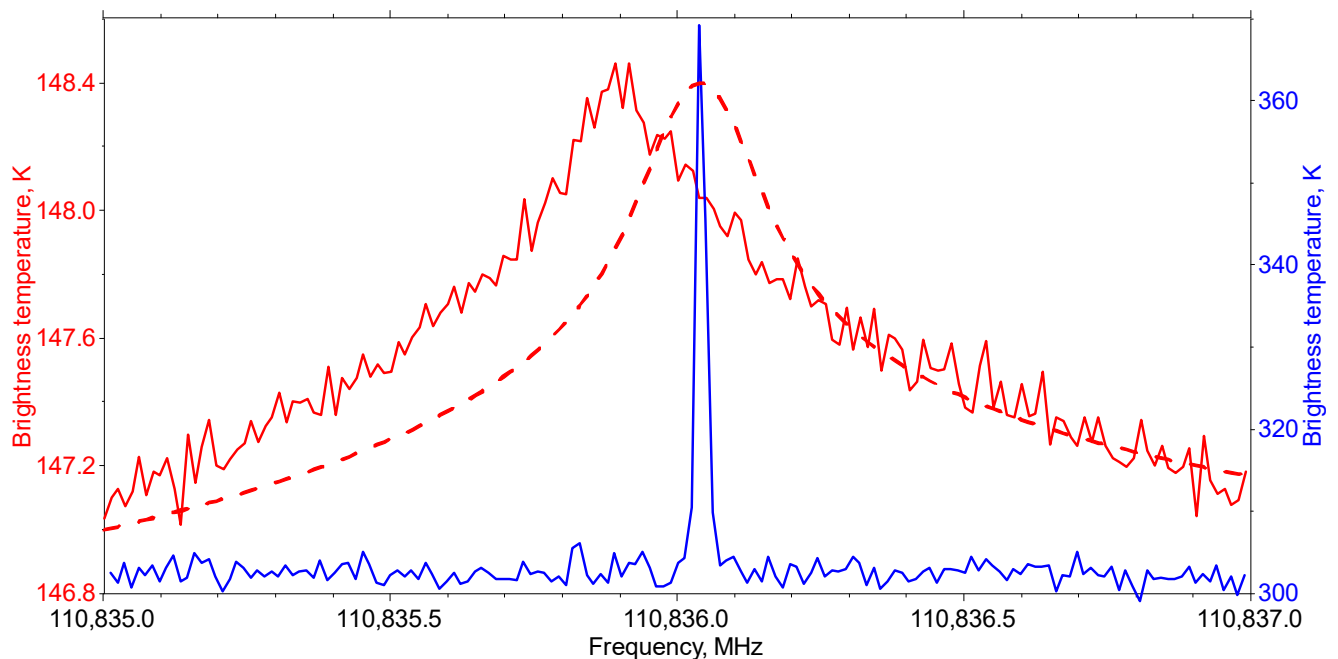


Figure 3. Red line: The brightness temperature spectrum of atmospheric ozone obtained by averaging data measured on 15–29 April 2019 at a tropospheric attenuation coefficient of <2.5 . Blue line: the spectrum of reference monochromatic signal at the frequency of 110,836.040 MHz. Red dashed line: the example of simulated spectrum of atmospheric ozone with the central frequency of 110,836.040 MHz.

As mentioned above, the reference signal was initially generated by R&S[®]SMB100A with subsequent multiplication by 10. It was sent to the input of the ozonometer and went through all stages of processing like a signal coming from the atmosphere, so both spectra shown in Figure 1 are from the digital spectrum analyzer. One can see from this figure that the center frequency of the ozone spectrum was less than the laboratory value, with the difference being more than 100 kHz.

The results of theoretical estimations of meridional wind influence on the center frequency of the ozone line are shown in Figure 4. It can be seen that, in all seasons, a possible Doppler shift by this wind did not exceed ~ 4 kHz, whereas the mean absolute shift was ~ 1.5 kHz that was essentially less than the spectral resolution of the measured data. Thus, taking into account the north orientation of measurements, we can suppose that, in our case, the horizontal wind has little influence on the determination of the resonance frequency of the ozone line.

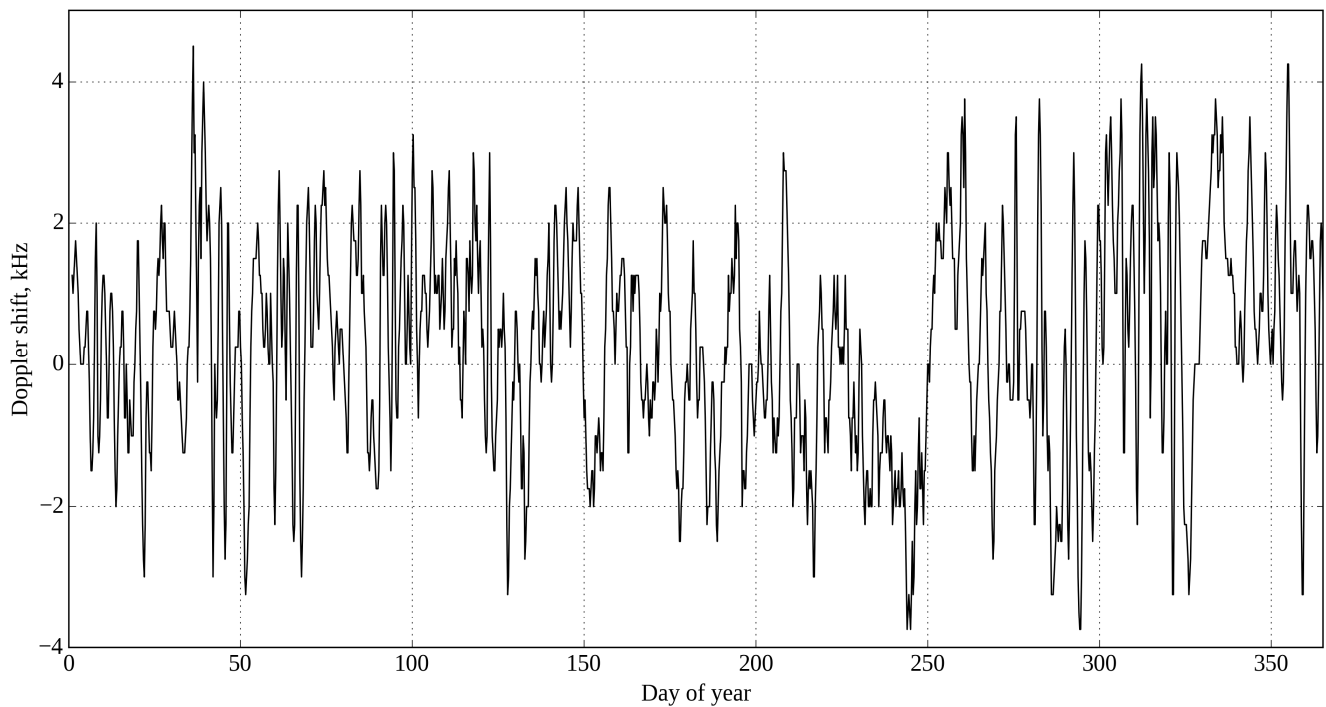


Figure 4. Doppler shift of the center frequency of ozone line by meridional wind over Nizhny Novgorod during a year.

Figure 5 depicts estimates of the ozone line center frequency corresponding to four sets of 1-day averaged spectra. All sets were obtained from the same dataset of 1 h averaged spectra, but at different values of the filtering parameter threshold.

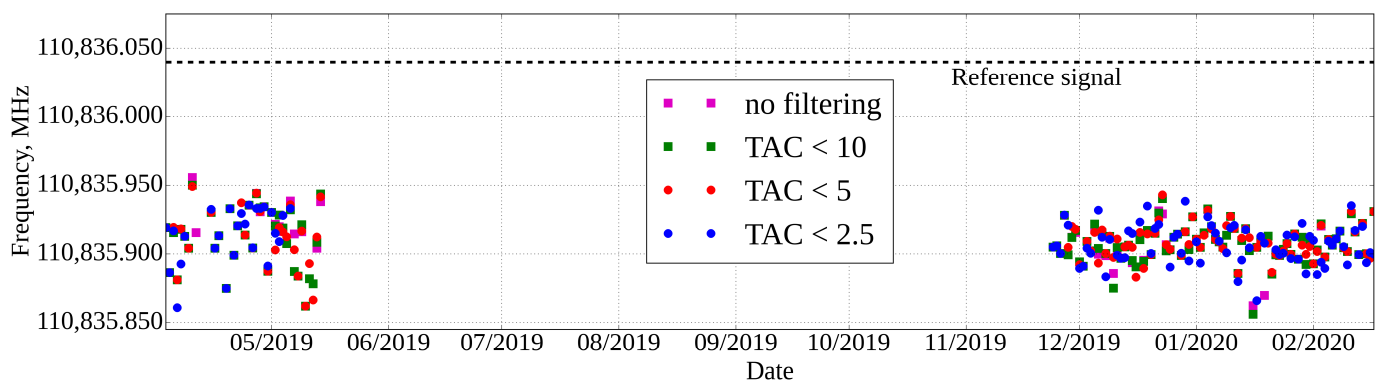


Figure 5. Center frequency of the ozone line estimated from four ensembles of 1-day averaged spectra corresponding to different tropospheric attenuation coefficient (TAC) thresholds.

The statistical processing of these datasets, first, revealed that the mean values are very close and differ by less than 1 kHz (see Table 2). The same is true for the standard deviation values.

Table 2. Mean frequencies and standard deviations for datasets shown in Figure 5.

Dataset	Mean	Standard Deviation
no filtering	110,835.908475 MHz	15.733 kHz
TAC < 10	110,835.908545 MHz	16.074 kHz
TAC < 5	110,835.909450 MHz	15.217 kHz
TAC < 2.5	110,835.908585 MHz	15.864 kHz

Thus, we can conclude, first, that like in the case of the Doppler shift, tropospheric absorption has little influence on the result. Second, the resonance frequency of the ozone transition $J = 6_{1,5}-6_{0,6}$ was $110,835.909 \pm 0.016$ MHz that was 131 ± 16 kHz less than the one measured in the laboratory.

5. Discussion

The comparison with data in Table 1 showed that the found position of the O₃ line is consistent with Forkman et al. [12], i.e., we confirmed the previously discovered shift from the generally accepted value of 110,836.040 MHz. As noted, Forkman et al. [12] used the coincidence of the measured and simulated spectra of the CO line as a reference point. In our case, we could not analogously use other atmospheric lines, so we resolved the issue by precision laboratory measurements of frequency conversion inside with our spectroradiometer when a signal propagates from the antenna to the digital spectrum analyzer. Therefore, the existence of O₃ line shift has been established with high accuracy. Surprisingly, our result is close to the results of the early semiempirical calculations [13,15,16] performed more than 40–50 years ago, whereas there is a marked difference (up to 360 kHz [19,20]) from modern model calculations. Note that the only laboratory measurements of this important O₃ line were made more than 50 years ago [13]. Therefore, new measurements are long overdue.

Let us discuss possible applications where knowledge about precise position of this ozone line can be potentially important. One can assume at least two directions. First, the found resonance frequency of the ozone transition $J = 6_{1,5}-6_{0,6}$ can be used as a reference point to test and validate modern semiempirical and quantum chemical methods and models. In particular, comparison of the model results for this ozone transition with our value and extrapolation to other frequency ranges can help to estimate calculation errors of the following ozone rotation lines or other molecules. Second, the development of radio-electronic components (first of all, their minituarization and improving sensitivity) opens up new opportunities in microwave remote sensing of the middle atmosphere. It not only will boost the use of ground-based and airborne (including UAVs) measurements, but also will allow more elaborate measurements that utilize the effects of smaller amplitudes. The line in question can be used for the retrieval of mesospheric ozone and the corresponding wind profile in a manner similar to [14]. This needs precise measurements of brightness temperature spectra in narrow bands near the line central frequency with high spectral resolution (up to 1 kHz). The precision the central frequency value should exceed the characteristic Doppler shift. The inaccuracy in the frequency leads to systematic error in the mesospheric values ozone profile and disrupts the corresponding wind retrieval. Thus, our result is crucial for these tasks.

6. Conclusions

We have performed long-term ground-based passive measurements of downwelling atmospheric radiation at ~110.836 GHz with high technical accuracy and spectral resolution. Processing of the obtained brightness temperature spectra gave the resonance frequency of ozone rotational transition $J = 6_{1,5}-6_{0,6}$ of $110,835.909 \pm 0.016$ MHz that was 131 ± 16 kHz less than the laboratory measured one. Therefore, the previously discovered shift from the generally accepted value has been established with high precision. Nevertheless, new laboratory measurements of this O₃ line important for the atmosphere are needed and long overdue.

In conclusion, note that this paper confirms the emerging trend that the modern capabilities of environmental research equipment have reached a level allowing measurements of the accuracy and solution of the problems that were earlier possible only in the laboratory.

Author Contributions: Conceptualization, A.A.K. and M.Y.K.; methodology, A.A.K., M.Y.K. and M.V.B.; software, M.V.B.; validation, A.A.K. and M.Y.K.; formal analysis, A.A.K., M.V.B. and M.Y.K.; investigation, A.A.K., M.Y.K., M.V.B., A.A.S., N.K.S., L.M.K. and A.M.F.; resources, A.A.K., V.G.R. and A.A.S.; writing—original draft preparation, M.Y.K., A.A.K. and M.V.B.; writing—review and editing, V.G.R., A.A.S., N.K.S., L.M.K. and A.M.F.; visualization, M.V.B.; supervision, A.M.F.; project administration, M.Y.K.; funding acquisition, M.Y.K. All authors have read and agreed to the published version of the manuscript.

Funding: This work was supported by the Russian Science Foundation under grant No. 22-12-00064, <https://rscf.ru/project/22-12-00064/>, accessed on 21 April 2023.

Data Availability Statement: Data presented in this study are available on request from the corresponding author (kulm@ipfran.ru).

Conflicts of Interest: The authors declare no conflict of interest. The funders had no role in the design of the study; in the collection, analyses, or interpretation of data; in the writing of the manuscript; or in the decision to publish the results.

References

1. Penfield, H.; Litvak, M.M.; Gottlieb, C.A.; Lilley, A.E. Mesospheric ozone measured from ground-based millimeter wave observations. *J. Geophys. Res.* **1976**, *81*, 6115–6120. [[CrossRef](#)]
2. Krasil'nikov, A.A.; Kulikov, M.Yu.; Kukin, L.M.; Ryskin, V.G.; Fedoseev, L.I.; Shvetsov, A.A.; Belikovich, M.V.; Bolshakov, O.S.; Schitov, A.M.; Mikhailovskiy, V.L.; et al. Mobile spectroradiometric complex for middle atmosphere ozone soundings. *Radiophys. Quantum Electron.* **2014**, *56*, 628–637. [[CrossRef](#)]
3. Palm, M.; Hoffmann, C.G.; Golchert, S.H.W.; Notholt, J. The ground-based MW radiometer OZORAM on Spitsbergen—Description and status of stratospheric and mesospheric O₃ measurements. *Atmos. Meas. Tech.* **2010**, *3*, 1533–1545. [[CrossRef](#)]
4. Fernandez, S.; Murk, A.; Kämpfer, N. GROMOS-C, a novel ground-based microwave radiometer for ozone measurement campaigns. *Atmos. Meas. Tech.* **2015**, *8*, 2649–2662. [[CrossRef](#)]
5. Rodgers, C.D. *Inverse Methods for Atmospheric Sounding: Theory and Practice*; World Scientific: Singapore, 2000; p. 240.
6. Steinbrecht, W.; Froidevaux, L.; Fuller, R.; Wang, R.; Anderson, J.; Roth, C.; Bourassa, A.; Degenstein, D.; Damadeo, R.; Zawodny, J.; et al. An update on ozone profile trends for the period 2000 to 2016. *Atmos. Chem. Phys.* **2017**, *17*, 10675–10690. [[CrossRef](#)]
7. Hocke, K.; Kämpfer, N.; Feist, D.G.; Calisesi, Y.; Jiang, J.H.; Chabrilat, S. Temporal variance of lower mesospheric ozone over Switzerland during winter 2000/2001. *Geophys. Res. Lett.* **2006**, *33*, L09801. [[CrossRef](#)]
8. Moreira, L.; Hocke, K.; Navas-Guzmán, F.; Eckert, E.; von Clarmann, T.; Kämpfer, N. The natural oscillations in stratospheric ozone observed by the GROMOS microwave radiometer at the NDACC station Bern. *Atmos. Chem. Phys.* **2016**, *16*, 10455–10467. [[CrossRef](#)]
9. Kulikov, M.Yu.; Krasil'nikov, A.A.; Shvetsov, A.A.; Fedoseev, L.I.; Ryskin, V.G.; Kukin, L.M.; Mukhin, D.N.; Belikovich, M.V.; Karashtin, D.A.; Skalyga, N.K.; et al. Simultaneous ground-based microwave measurements of the middle-atmosphere ozone and temperature. *Radiophys. Quantum Electron.* **2015**, *58*, 409–417. [[CrossRef](#)]
10. Belikovich, M.V.; Ryskin, V.G.; Kulikov, M.Y.; Krasilnikov, A.A.; Shvetsov, A.A.; Feigin, A.M. Microwave observations of atmospheric ozone over Nizhny Novgorod in winter of 2017–2018. *Radiophys. Quantum Electron.* **2021**, *63*, 191–206. [[CrossRef](#)]
11. Rüfenacht, R.; Murk, A.; Kämpfer, N.; Eriksson, P.; Buehler, S.A. Middle-atmospheric zonal and meridional wind profiles from polar, tropical and midlatitudes with the ground-based microwave Doppler wind radiometer WIRA. *Atmos. Meas. Tech.* **2014**, *7*, 4491–4505. [[CrossRef](#)]
12. Forkman, P.; Christensen, O.M.; Eriksson, P.; Billade, B.; Vassilev, V.; Shulga, V.M. A compact receiver system for simultaneous measurements of mesospheric CO and O₃. *Geosci. Instrum. Method. Data Syst.* **2016**, *5*, 27–44. [[CrossRef](#)]
13. Lichtenstein, M.; Gallagher, J.J.; Clough, S.A. Millimeter wave spectrum of ozone. *J. Mol. Spectrosc.* **1971**, *40*, 10–26. [[CrossRef](#)]
14. Gora, E.K. Rotational spectrum of ozone. *J. Mol. Spectrosc.* **1959**, *3*, 78–99. [[CrossRef](#)]
15. Depannemaeker, M.J.C.; Duterage, B.; Bellet, M.J. Systematic calculations of rotational spectra of normal and substituted (¹⁸O in place of ¹⁶O) ozone molecules. *J. Quant. Spectrosc. Radiat. Transfer.* **1977**, *17*, 519–530. [[CrossRef](#)]
16. Kolbe, W.F.; Buscher, H.; Leskovar, B. Microwave absorption coefficients of atmospheric pollutants and constituents. *J. Quant. Spectrosc. Radiat. Transfer.* **1977**, *18*, 47–64. [[CrossRef](#)]
17. The HITRAN Database. Available online: <https://hitran.org> (accessed on 10 January 2023).
18. JPL Molecular Spectroscopy. Available online: <https://spec.jpl.nasa.gov/> (accessed on 10 January 2023).

19. GEISA Spectroscopic Database. Available online: <https://cds-espri.ipsl.upmc.fr/etherTypo/index.php?id=950&L=1> (accessed on 10 January 2023).
20. Spectroscopy and Molecular Properties of Ozone. Available online: <https://smpo.iao.ru> (accessed on 10 January 2023).
21. Rosenkranz, P.W. Line-by-Line Microwave Radiative Transfer (Non-Scattering). Remote Sens. Code Library. 2017. Available online: http://cetemps.aquila.infn.it/mwrnet/lblmrt_ns.html (accessed on 10 January 2023).
22. Krasil'nikov, A.A.; Kulikov, M.Y.; Kukin, L.M.; Ryskin, V.G.; Fedoseev, L.I.; Shvetsov, A.A.; Bolshakov, O.S.; Shchitov, A.M.; Feigin, A.M. Automated Microwave Radiometer for Measuring the Atmospheric Ozone Emission Line. *Instrum. Exp. Tech.* **2017**, *60*, 271–273. [[CrossRef](#)]
23. Krasil'nikov, A.A.; Kulikov, M.Y.; Ryskin, V.G.; Fedoseev, L.I.; Shvetsov, A.A.; Bozhkov, V.G.; Bol'shakov, O.S. Calibration system for microwave radiometers based on modulator-calibrator. *Instrum. Exp. Tech.* **2017**, *60*, 701–704. [[CrossRef](#)]
24. Aura MLS. Available online: <https://mls.jpl.nasa.gov/eos-aura-mls> (accessed on 10 January 2023).
25. de Grandpre, J.; Beagley, S.R.; Fomichev, V.I.; Griffioen, E.; Mc-Connell, J.C.; Medvedev, A.S.; Shepherd, T.G. Ozone climatology using interactive chemistry: Results from the Canadian Middle Atmosphere Model. *J. Geophys. Res.-Atmos.* **2000**, *105*, 26475–26491. [[CrossRef](#)]
26. Scinocca, J.F.; McFarlane, N.A.; Lazare, M.; Li, J.; Plummer, D. The CCCma third generation AGCM and its extension into the middle atmosphere. *Atmos. Chem. Phys.* **2008**, *8*, 7055–7074. [[CrossRef](#)]

Disclaimer/Publisher's Note: The statements, opinions and data contained in all publications are solely those of the individual author(s) and contributor(s) and not of MDPI and/or the editor(s). MDPI and/or the editor(s) disclaim responsibility for any injury to people or property resulting from any ideas, methods, instructions or products referred to in the content.